

## Original papers

# Numerical and experimental vibration analysis of olive tree for optimal mechanized harvesting efficiency and productivity



Hamidreza Hoshyarmanesh<sup>a,\*</sup>, Hamid Rezvani Dastgerdi<sup>b</sup>, Mojtaba Ghodsi<sup>c</sup>, Rasoul Khandan<sup>d</sup>, Kourosh Zareinia<sup>a</sup>

<sup>a</sup> Project neuroArm, Health Research Innovation Centre, Department of Clinical Neurosciences, University of Calgary, Canada

<sup>b</sup> School of Mechanical Engineering, University of Western Australia, Perth, Australia

<sup>c</sup> Department of Mechanical Engineering, Sultan Qaboos University, Muscat, Oman

<sup>d</sup> Department of Material Engineering, Loughborough University, Leicestershire, UK

## ARTICLE INFO

## Article history:

Received 24 June 2016

Received in revised form 13 November 2016

Accepted 16 November 2016

Available online 27 November 2016

## Keywords:

Numerical vibration analysis

Olive tree structure

Trunk shaker

Harvesting percentage

Productivity

## ABSTRACT

A 3D model of a middle-size olive tree has been analyzed considering various shaking conditions by using an attached trunk shaker to improve the harvesting rate as regards the critical nodal acceleration and displacement. The effects of shaking frequency, loading type as well as temperature and loading height were simulated and investigated on olive-stem-twig joint rupture. Comparing the results of finite element modal analysis in ABAQUS 6.10 with those of field experiments, utilizing a hydraulic eccentric-mass trunk shaker, exhibits less than 5% deviation at frequencies between 10 and 25 Hz at the first four vibration modes with damping ratio of 16–30%. The experiments and simulations show the maximum harvested quantity of sample middle-size olive trees is 92% and 96%, respectively. It is acquired at  $f = 20$  Hz,  $T = 28$  °C for 45% moisture content of wood in late November 2012, without chemicals. The optimized mechanical harvesting yielded the lower number of workers, time saving (~12 tree/h), and to improve the obtained productivity (293 kg/h). The results imply that accurate 3D analysis of mechanized olive harvesting can be an efficacious solution to obtain desired parameters and optimal efficiency, which is comparable to manual method.

© 2016 Elsevier B.V. All rights reserved.

## 1. Introduction

Mechanized harvesting process has drawn significant attention in recent decades as an unavoidable utility in order to cost reduction, time saving and speed up delivery of important agricultural crops like olives, cherry, apricot, almond, etc. Unaffordable and time-consuming hand picking is the main problem in traditional olive harvesting. In last decades, approaching to mechanized harvesting methods has been considerably grown. Although mechanized harvest approaches are widely implemented in many fields and orchards, less than 75% (per tree) of all crops are currently collected mechanically (Castro-García et al., 2014; Yousefi and Gholiyan, 2013) and therefore, there is still need to hire labors to pick the remainders on the tree. So, it is still needed to study the maximum efficiency of fruit harvesting by a more accurate modeling and analysis without abscission agents. In spite of the higher Harvesting Percentage (HP) reported for branch shaking machines or manual branch shakers (above 78%) (Yousefi et al., 2010), those

methods are not time-efficient, cost-effective and protective against limb breakage as much as hydraulic trunk shaker. “Trunk Shaker” is one of the most important olive harvesting devices due to its simple eccentric rotational mass, variety of vibration patterns, more conventional usage compared with other methods, capability of linear or orbital loading and installing on traditional tractors (Sola-Guirado et al., 2014). Taking into account that mechanized harvesting increases the fruit damage index (Castro-García et al., 2015), the analysis and optimization process should facilitate the vibration transmission to the stem nodes on upper branches and protect the tree against breakage, rupture or delamination. The main objective of the present study is determining the optimum parameters of mechanized hydraulic olive harvesting in well-pruned orchards of Northern Iran to reach the maximum HP and productivity, simultaneously. The productivity is measured as collected fruit per hour (kg/h) per a single worker regarding harvesting period of each tree in a sample orchard. Conventional harvesting systems have some noticeable disadvantages like low HP, fruit bruising, stalk breakage, root and bark damages, leaf falling due to chemicals, etc. Therefore, an exhaustive optimization analysis of mechanized olive harvesting, which takes into account the

\* Corresponding author.

E-mail address: [hamidreza.hoshyarman@ucalgary.ca](mailto:hamidreza.hoshyarman@ucalgary.ca) (H. Hoshyarmanesh).

most technical effective parameters, is promisingly expected to solve the main problems of conventional trunk shakers (Gezer, 1999). As many publications in this field is assigned to experimental studies (Farinelli et al., 2012a), simple 2D or 3D numerical simulations regardless of implementing temperature, wood orthotropic structure, humidity, linear loading, etc. (Bentaher et al., 2013; El-Awady et al., 2008), analysis of citrus trees (Savary et al., 2010; Yung and Fridley, 1975), investigation of different shaking methods (Yousefi et al., 2010), and study of detachment forces (Farinelli et al., 2012b), there is no reference in this field to be addressed considering the most effective parameters, entirely. In present research, Finite Element Analysis (FEA) is utilized to investigate the harvesting productivity of a real 3D structure with respect to the temperature and moisture-dependent behavior of elastic constants, load direction (linear and orbital) and loading height. The obtained results are compared with the experimental results in a designated well-pruned orchard as the representative for all similar circumstances to evaluate the average harvesting productivity.

## 2. Literature review

Adrian and Fridley (1965) investigated the vibrational behavior of a tree based on an unbalanced eccentric sinus loading, basic theory of vibrations and design criteria for various shakers in 1965. Yung and Fridley (1975) simulated an entire model of a tree and used FEA to study the vibrations in the whole system. In their report, mechanical properties of tree components were supposed to be elastic, homogenous and isotropic. At the same time, Keçecioglu (1975) focused on an inertial mass shaker for olive harvesting and reported that olive tree should be vibrated 10 s at frequencies of 20–28 Hz with the wave amplitude of 20–30 mm to achieve the best harvesting efficiency. Near a quarter century later, Metzidakis (1999) reported the vibration effects on mechanical olive harvesting and inferred that mechanical vibration is not effective by itself to harvest more than 50% of total mass. Energy consumption of different shakers under various conditions was reported by Horvath and Sitkei (2001) who investigated the soil mass and damping properties in “tree-soil” vibration system. Sessiz and Özcan (2006) reported the efficiency of olive harvesting less than 50% using a pneumatic shaker without any chemicals and about 96% using chemical solutions at 24 Hz frequency. James et al. (2006) presented a model of tree in 2006 with specified dynamic characteristics of trunk and branches and showed the damping effect on reduction of tree oscillating movement. El-Awady et al. (2008) simulated a simple 3D branch of an olive tree in SAP2000 and analyzed its dynamic behavior regarding the mass and stiffness matrices. With respect to their results, top parts of an olive tree respond to frequencies near 22 Hz and displacement of 10 cm, while bottom portion does not react easily to frequencies above 14 Hz with less harvesting efficiency. They reported that loading height of 40 cm above the ground would have excited most branches and enhanced harvesting process. Green and Evans (2008) studied the effect of temperature between –26 and +66 °C and the Moisture Content (MC) on elasticity modulus of dry and wet wood and achieved the linear relationship between the increases of elasticity modulus with decrease of temperature. Dahmen et al. (2010) measured non-homogeneous engineering constants of anisotropic olive wood plates using air-coupled transducers generated Lamb wave and ultrasonic bulk wave. In the research work performed by Cicek et al. (2010) olive trees were harvested by four different methods. From the data obtained during a two-year period, the mechanical bough shaker + wood stick method was determined to be the one with the highest capacity. Savary et al. (2010) designed and optimized a canopy shaker and

studied dynamic simulation of citrus trees beside field experiments. They determined the mechanical properties of the citrus tree wood under the assumption that it is isotropic in nature. Then, the acceleration data from the simulation were compared against the experimental data at 3–4 Hz frequencies. It is notable that the harvesting efficiency and productivity were not considered as their output results. Yousefi et al. (2010) compared pneumatic comb harvesting machine with branch shaking machine and hand picking. They believed that the mechanized method of harvesting has greatly improved the timeliness of operation, and the productivity of the labor. Moreover, productivity reduced as the fruit size and weight decreased. Di Vaio et al. (2012) and Famiani et al. (2014) determined the efficiency of mechanical olive harvesting with trunk shaker in southern Italy. The mechanical harvesting yield led to some advantages of low number of workers and reduced time for the operation which allowed a high productivity to around 302 kg/h per worker for ‘Ortice’ cultivar. Castro-García et al. (2014) studied and measured fruit detachment force (FDF) and tree geometrical characteristics by three triaxial piezoelectric accelerometers. In their work, HP varied from 56 to 87%. Although increased vibration power applied to trees for high level of canopy vibration improves harvesting efficiency, Castro-García et al. (2015) showed that it also implies an increase in fruit damage index especially in larger fruits with a positive linear relationship. One remarkable study was the one reported by Bentaher et al. (2013) who studied the stem shaking conditions in the mechanical harvesting of “Chemlali” olive fruits—the main variety in Tunisia—by undertaking a FE numerical modeling. They modeled an olive tree by 3D beams; Each beam had two nodes and 6 degrees of freedom for each node; The structure was built by 560 elements and 561 nodes. The Orbital and multidirectional (not linear) loading were tested and the excitatory force equation was developed as a function of the unbalanced mass, eccentricity and rotational frequency. Orbital loading was determined as preferable choice due to its higher reaction force. However, they did not perform any functional practice to compare their obtained results with their expected experiments. These inaccurate outputs cannot be justified regarding the experimental displacement and optimal productivity. A few papers are presently published on 3D modeling of olive tree structures. This study is significantly considering the important effective parameters such as anisotropic nature of olive wood, real 3D simulation, temperature and moisture-dependent behavior of elastic constants, load direction (linear and orbital), loading height, and harvesting productivity, together and simultaneously. Wood temperature and MC were measured using a non-contact digital infrared thermometer (DT-8380) and a pin-type Wagner wood moisture meter, respectively.

## 3. Materials and methods

### 3.1. Olive tree structure

The design of mechanized hydraulic harvesting machines is based on transmission of mechanical waves into the boughs as well as main branches, limbs, twigs, stems and nodes, which leads to orbital movement of fruits. It finally results in stem-twig or stem-fruit detachment and fruit dropping down (Di Vaio et al., 2013). The variable force applied to the fruit creates a momentum results in failure stress riser at the stem node, and if the force is large enough, the fruit will be detached. Attachment force of the stem to small branches depends on the different stages of fruit ripening. As the fruit further ripens, the harvest quantity rate grows highly (Ferguson et al., 2010). Using chemicals at harvesting time attenuates the attachment forces, causes vigorous mechanical harvesting and facilitates the fruit detachment. However, the use

of chemicals increases harvesting rate, it might lead to falling the leaves and blossoms in the next period of blooming (Hedden and Churchill, 1984). Not using abscission agents, the damage introduced to trees and fruits could be reduced greatly (Yousefi et al., 2010; Yousefi and Gholiyan, 2013). In this research, we focused on mechanized harvesting of olive trees based on mean values of mechanical parameters for the samples reported in Table 1. The selected orchard located in Northern Iran (latitude 28° N and longitude 57° E) includes mostly 6–8 years of age *Mari* Cultivar specimens. The trees are trained in such that the branches are spaced 5–10 cm apart at their insertion point. They emerge from the trunk at least 1.2 m above ground level to allow mechanical harvesting. The branches have been spread out by supporting them on sticks or encircling them with a hoop. This training method causes a strong and functional framework. Vibratory force is exerted on the trunk by a hydraulic inertial trunk shaker with the 40 kW maximum power, un-balanced mass of 4–30 kg, and working frequency of 10–25 Hz.

### 3.2. Modeling and simulation

#### 3.2.1. 3D olive tree with trunk shaker

A 3D model of a middle-size olive tree was modeled in Autodesk Inventor Pro., regarding the principal parameters written in Table 1. The model consists of a bough, three main branches, four subshrubs and olive-stem-twig joints. Canopy volume and branches were modeled at an intermediate state between a quite pruned and a full foliage tree. The base was fully constrained and a shaker equipped with 70 kg eccentric mass was attached to the trunk, which is able to increase to 100 kg. Partitioning the model made definition of 12168 stem nodes overall the deformable body. We select four numbered stem nodes (a–d) at different directions and heights relative to the trunk axis as shown in Fig. 1. The shaker inserted in 3D model as an analytical rigid body “tie” elements (considering its geometry, mass, and centrifugal loading to simulate the real conditions) determines the position of applied orbital/linear loading and might be effective in external damping. The ignored grabbing elastic pad of the shaker is assumed hard enough such that it didn’t consider as a true structural damper at low frequencies. It is utilized solely as a protective layer to prevent bark delamination. The tree is considered as trunk, main branches, small branches, and twigs as an integrated unique structure. The “olive + stem” is modeled as a tied pendulum sways around the specified node with respect to its mass and consequently its acceleration which induces the nodal reaction force ( $R$ ) and normal stress ( $\sigma$ ) at the connection node. This reaction force is finally compared with the required FDF.

#### 3.2.2. Orthotropic properties of olive wood

Olive wood is composed of a series of co-centric cylindrical layers. As a non-isotropic material, it includes the bark layer, cambium cell layer, sapwood and heartwood, which leads to a cylindrical symmetry. To study the mechanical properties of olive wood, three orthogonal elastic axes of symmetry are considered in longitudinal, radial and tangential directions as demonstrated in Fig. 2 (Saglam and Aktas, 2005). Elastic and strength constants of orthotropic materials such as olive wood are variable along three directions. Eq. (1) defines the Hooke’s law for orthotropic materials ( $\sigma = C\varepsilon$ ) where the stress components ( $\sigma_i$ ) are linear variables of strains ( $\varepsilon, \gamma_j$ ) related together by the elastic stiffness values  $C_{ij}$ . In this equation,  $\varepsilon$  and  $\gamma$  represent the normal and shear strains, respectively. Hence, there will be nine independent elastic stiffness constants. According to the previous studies, the mean value of the elastic constants of the olive wood (in GPa) is defined in Eq. (1) (Dahmen et al., 2010).

$$\begin{Bmatrix} \sigma_1 \\ \sigma_2 \\ \sigma_3 \\ \sigma_4 \\ \sigma_5 \\ \sigma_6 \end{Bmatrix} = \begin{bmatrix} 4.35 & 3.03 & 2.59 & 0 & 0 & 0 \\ 3.03 & 4.51 & 2.08 & 0 & 0 & 0 \\ 2.59 & 2.08 & 10.8 & 0 & 0 & 0 \\ 0 & 0 & 0 & 1.05 & 0 & 0 \\ 0 & 0 & 0 & 0 & 1.12 & 0 \\ 0 & 0 & 0 & 0 & 0 & 0.95 \end{bmatrix} \begin{Bmatrix} \varepsilon_1 \\ \varepsilon_2 \\ \varepsilon_3 \\ \gamma_1 \\ \gamma_2 \\ \gamma_3 \end{Bmatrix} \quad (1)$$

If the elastic behavior of olive wood is expressed in terms of engineering elastic constants according to Eq. (2), where  $E_p = E_R = E_T$  is the equivalent Young’s modulus in  $RT$  plane,  $G_p = G_{RT}$  is the shear modulus in  $RT$  plane, and  $G_t = G_{RL} = G_{TL}$  is the equivalent shear modulus related to the perpendicular  $RL$  and  $TL$  planes, the wood could be considered as a cylindrical orthotropic body and simplified relation for a linear elastic transversely isotropic material would be written as: (Bower, 2009; Bucur, 2006; Mascia and Lahr, 2006).

$$\{\varepsilon_m\} = [S_{mn}]\{\sigma_n\} \quad (2)$$

In Eqs. (3)–(6),  $\nu_{ij}$  is the Poisson’s ratio in  $ij$  plane. The transverse displacement is considered constant across the thickness, and in-plane displacement is linear.

$$S = \begin{bmatrix} 1/E_p & -\nu_p/E_p & -\nu_{tp}/E_t & 0 & 0 & 0 \\ -\nu_p/E_p & 1/E_p & -\nu_{tp}/E_t & 0 & 0 & 0 \\ -\nu_{pt}/E_p & -\nu_{pt}/E_p & 1/E_t & 0 & 0 & 0 \\ 0 & 0 & 0 & 1/G_t & 0 & 0 \\ 0 & 0 & 0 & 0 & 1/G_t & 0 \\ 0 & 0 & 0 & 0 & 0 & 1/G_p \end{bmatrix} \quad (3)$$

$$\nu_{TR} = \nu_{RT} = \nu_p, \quad \nu_{LR} = \nu_{LT} = \nu_{tp}, \quad \nu_{RL} = \nu_{TL} = \nu_{pt} \quad (4)$$

$$G_p = E_p/2(1 + \nu_p) = C_{66}, \quad G_t = C_{44} \quad (5)$$

$$\nu_{pt} = \nu_{tp} \cdot \frac{E_p}{E_t} \quad (6)$$

The transverse shear strains across tree layers next to each other are assumed linearly dependent on each other as it is shown for the in-plane composite simulation. If the in-plane stress gets too large, then fiber breakage or material yield occurs. However, normally before the in-plane stresses exceed the fiber breakage point, interlaminar shear stress failure occurs when one layer slips tangentially relative to another (Khandan et al., 2012a,b). The elastic constants of wood depend on temperature (affects the humidity) and reduce slightly as the temperature increases due to dilatation of crystalline cellulose. The relative change in modulus of elasticity ( $\delta E$ ) from 23 °C can be expressed as Eq. (7) for green olive wood (45% MC) (Green and Evans, 2008).

$$\delta E_L(\%) = -0.3216T + 7.4475, \quad 0 < T < 30 \text{ }^\circ\text{C} \quad (7)$$

As illustrated in Fig. 3, the intensity of temperature influence on the elastic modulus of olive wood would be greater as the moisture increases (Green and Evans, 2008; Mascia and Cramer, 2009; Mascia, 2003).

#### 3.2.3. Vibrational dynamic behavior

The model was meshed and simulated based on the real parameters in ABAQUS 6.10 using default 3D tetrahedral solid elements and actual ‘main branches’ to ‘trunk’ mass ratio. To model the tree as a vertical cantilever anchored at the section where it is protruding from a fixed ground, the trunk circular cross section was constrained at the end to restrain quite the root. Viscoelastic damping of wood and root-soil friction system was considered when modeling. The orbital load was applied in terms of pressure

**Table 1**  
Mean physical characteristics of 60 middle-size olive trees.

Parameter		Value [m]	Parameter	Value
Density @38% MC		950 [kg/m <sup>3</sup> ]	Poisson ratio	0.34
Trunk diameter	Thick section	0.18–0.25	Spherical crown volume	30–35 [m <sup>3</sup> ]
	Thin section	0.12–0.15		
Trunk height		1.1–1.5	Total fruit/tree	25–28.5 [kg]
Total height		3.2–3.7	Fruit mass/unit	3.0–3.5 [g]
Main branch length		1.15–1.62	Initial dia. of main branch	6.5–9.5 [cm]
Main branch diameter	Thick section	0.07–0.09	Olive-Stem-Twig detachment force	1.5–6.5 [N]
	Thin section	0.01–0.02		

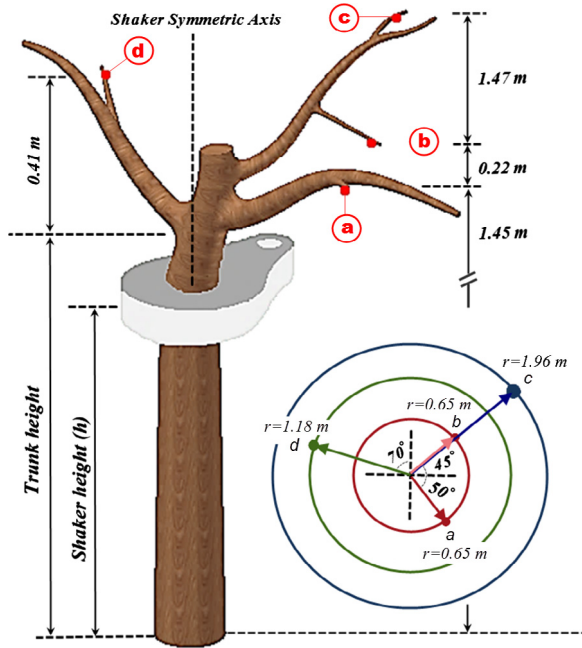


**Fig. 1.** 3D Model of an olive tree and olive-stem-twig joints at four locations; (a) node 5216, (b) node 5698, (c) node 6925, and (d) node 6274.

loading of  $P(\theta, f)$ ,  $\theta = 0-360^\circ$  to a cylindrical cavity on the shaker where driving shaft and unbalanced masses are assumed to be installed in practice. The shaker cylindrical cavity shown in Fig. 4 is composed of two semi cylinders: front and rear. Normal pressure  $P(\theta, f)$  was also applied to the model for linear loading considering only front semi-cylindrical cavity on the shaker towards ( $\theta = 0^\circ$ ) and away from ( $\theta = 180^\circ$ ) the trunk axis, intermittently.

When fruit trees are shaken, the damping losses may be very high, depending on the height above ground at which the shaker is attached. During shaking a given soil and root mass is taking part

into vibration. The soil, especially at large shaking amplitudes, has an increased damping ability and is the most important energy absorber of the whole system (Horvath and Sitkei, 2001). Applying a dynamic load to olive tree by trunk shaker causes vibration in bole, boughs, twigs and stems. The vibration induces momentum, acceleration and stress to stems and stem nodes. The tension and shear stress at stem nodes may overcome the FDF and the olive may be dropped down (Farinelli et al., 2012a). The optimized results of FEA are compared with those of field experiments and the optimized productivity is evaluated. Fruit weight (FW), harvest time and canopy drag are the most important factors distinguish the simulation results from what is obtained in reality. The olive trees of a well-pruned orchard show similar dynamic behavior in experiments due to their negligible differences in trunk diameter and crown size (Fig. 5). If the canopy is supposed as a sphere, the sphere volume is highly effective on HP. For small, stumpy and dense trees like olive tree, the principal vibration modes are influenced by the natural frequency of both trunk and branches (James et al., 2006). The olive tree is classified as a pretty dense structure (James et al., 2006; Erdoğan et al., 2003); thus its dynamic response is different from open-centered trees. A few different-size olive trees were modeled to investigate the morphology and dimension influence on tree dynamic behavior. Newton's second law defines motion characteristics of olive tree as an elastic structure having large degrees of freedom (DOF) as follows (Castro-García et al., 2008).

$$[M]\{\ddot{x}(t)\} + [C]\{\dot{x}(t)\} + [K]\{x(t)\} = \{f(t)\} \tag{8}$$

where  $[M]$ ,  $[C]$  and  $[K]$  are mass, damping and stiffness matrices, respectively, whereas  $\{\ddot{x}(t)\}$ ,  $\{\dot{x}(t)\}$  and  $\{x(t)\}$  are acceleration, velocity and displacement vectors for every node on the tree.  $\{f(t)\}$  is the time-varying applied force vector. Prior to study of forced excitation and damping, the natural frequency of the tree ( $\omega_n$ ) should be identified. Stimulation of the tree at  $f = 20-25$  Hz, resonates neither the tree structure nor the “olive + stem” system. However, the displacement of the twigs and small branches are noticeable in the excitation bandwidth compared to the tree with significantly larger

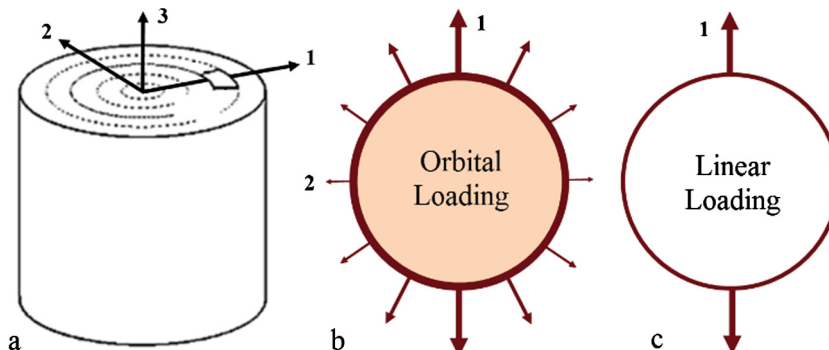


**Fig. 2.** (a) Orthogonal axes of symmetry in anisotropic structure of wood (Saglam and Aktas, 2005), (b) orbital harmonic loading in cross-sectional plane, and (c) linear loading.

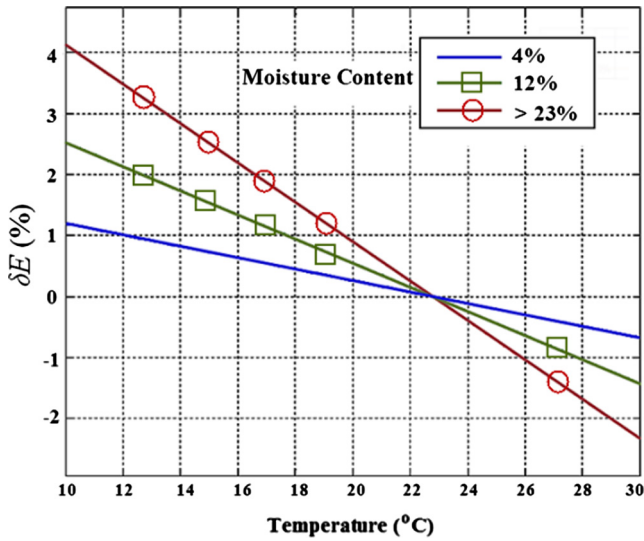


Fig. 3. Elastic modulus of olive wood vs. temperature and moisture content.

damping losses. Therefore, in the aforementioned range, we expect the olives oscillations and detachment with less trunk movement, as less displacement is more probable specifically in the lower part of the tree that might be accompanied by less root damage. Castro-García et al. (2008) considered vibration model of seventeen olive trees as damping harmonic oscillators in dense orchards under the forced vibration. Regarding the modal damping in forced vibration according to Rayleigh damping coefficients, the damping component proportional to the stiffness of the system was shown to be very reduced ( $\beta = 0.00045$ ), in agreement with the hypothesis of Sellier and Fourcaud (2005), who established an almost null value ( $\beta = 0.001$ ). Moreover, the damping component proportional to the inertia of the system had greater importance on the first two modes of vibration. Using an electromagnetic shaker, they found out an inverse linear relationship between damping ratio ( $\zeta$ ) and natural frequency ( $\omega_n$ ). In another words, the maximum power loss occurs in the mode with the lowest natural frequency. The elevated value of the initial damping could be explained because the mass of the soil that vibrates with the tree–soil system absorbs most of the energy according to the largest amplitudes in the tree–soil vibrating system (Horvath and Sitkei, 2001). Matrix [C] can be written as linear combination of [M] and [K], using the equivalent Rayleigh damping coefficients according to Eq. (9). It is an effective way to treat the damping value in systems with large DOF (Mascia, 2003). In general, the damping is not classical;  $R^T C R$  (R: modal matrix, C: damping matrix) is not a diagonal matrix, and the natural

frequencies, damping ratios, and modal vectors depend on the mass, stiffness, and damping matrices of the structure. However, a multi degree of freedom modal analysis for tree’s complex structure needs some simplifications consistent to reality to find heavily-damped modes. The function may be written as Eqs. (9) and (10) (Chowdhury and Dasgupta, 2003).

$$[C] = \alpha[M] + \beta[K] \tag{9}$$

$$\zeta_i = \frac{\alpha}{2\omega_i} + \frac{\beta\omega_i}{2} \tag{10}$$

Damping component proportional to the stiffness of the system ( $\beta$ : energy dissipation by hysteresis (Castro-García et al., 2008)) is obtained an almost null value compared with the damping component proportional to the inertia of the system ( $\alpha$ : energy dissipation through friction and resonance phenomena (Castro-García et al., 2008)) at several initial modes of vibration. To apply the proportional coefficients related to wood and root-soil-tree, the trunk is partitioned into two parts with different damping characteristics. Since the tree is fixed to the ground, the root-soil damping effect is applied indirectly to the nearest partition close to the ground which is as high as one fifth of the trunk height via setting the root alpha coefficient. According to Chowdhury and Dasgupta (2003), for the first portion of  $\zeta-\omega_n$  diagram, the curve shows non-linearity and beyond that the variations are linear. For some  $y = a/x + bx$ , the first term is  $a/x$  dominates at the initial stage. As  $x$  increases the value  $a/x$  approaches zero, while the term  $bx$  starts dominating the equation. Orthotropic wooden structure is placed in the non-linear range of damping at the investigated eigenmodes; so that damping ratio decreases as the frequency increases. At higher frequencies, the hysteresis (phase difference between trunk and upper branches) grows up in Rayleigh equation will be more conspicuous; indicating that aerodynamic damping has an even more important role in forced vibration vs. internal viscoelastic damping, where the amplitude of the movement is reduced (Castro-García et al., 2008). With reference to El-Awady et al. (2008), the middle parts of the tree have noticeable role in displacement and air drag. Since canopy volume and branches were modeled in this research at an intermediate state between a quite pruned and a full foliage tree, it is not a vase-shaped open centered crown and as a result is not freely exposed to airflow. Hence, regarding the effective role of middle-height branches, considering the proportional aerodynamic damping mechanism is not far from reality. Alpha and beta coefficients are determined by setting the damping ratios of the first and the fifth modes. FDF/FW ratio is a suitable index to determine the optimal time of simulation and harvesting duration, already studied by Farinelli et al. (2012b). The fruit mass increases during the ripening season, leads to

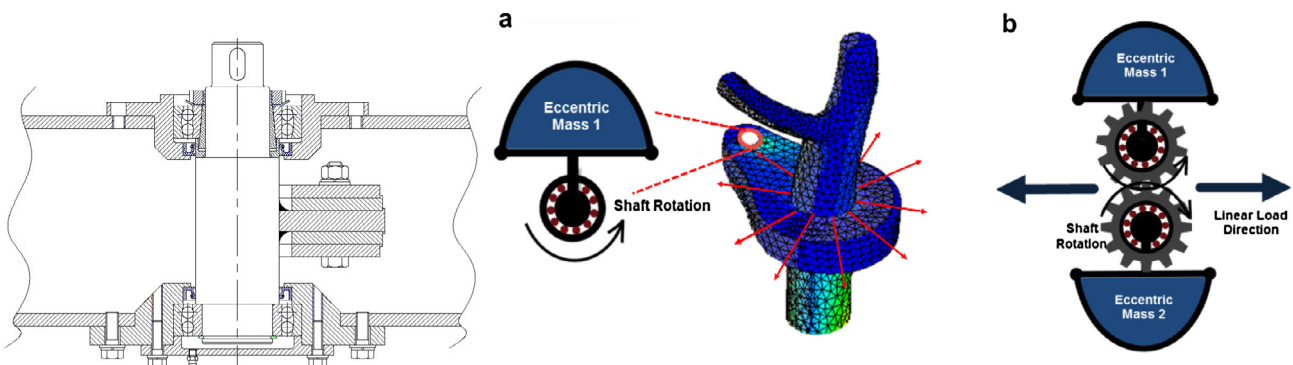


Fig. 4. (a) Orbital loading of the trunk shaker using rotation of one eccentric mass around the hydromotor shaft, and (b) linear loading by adding eccentric mass to the second rotating shaft.



Fig. 5. Over 70% of olive trees in the well-pruned orchard have similar characteristics. (Courtesy of an olive orchard in Northern Iran.)

reduction of FDF (Sessiz and Özcan, 2006). The mean value of FDF for olive fruit with 3.3 g average mass is measured 1.5–6.5 N. At first step, it is assumed that the shaker is located at a height of one meter above the ground and applies an eccentric orbital force at  $f = 20$  Hz. If we suppose the free load diagram as demonstrated in Fig. 6, using a simple acceleration analysis for a sample crucial node “a” ( $\ddot{x}_2 = 2.443e + 2$  and  $\ddot{y}_2 = 1.873e + 2$  m/s<sup>2</sup>), the minimum supporting load at olive stem-twig joints would be calculated as 2.7 N, which is probably insufficient to detach the fruit by applying unbalanced rotational loading. Since, it is not possible to model all fruit nodes, we focus on the nodes closer to the trunk with less harvesting success in practice (olives that remain on the tree after harvesting).

#### 4. Field experiments

The trunk is grabbed by a developed hydraulic-powered trunk shaker which is driven by a traditional tractor. The constituents of mechanism consist of two hydraulic radial piston pump, oil tank, hydromotor, hydraulic grip cylinders, four flow control valves, three pressure reducer valves, three directional control valves, column, main link, shaker frame, movable jaws and other accessories needed for assembling as shown in Fig. 7. The proposed shaker accommodates two rotating normal axes parallel to the trunk coupled to the hydromotor shaft which rotate reversely using two spur gears in mesh. This mechanism exerts orbital and linear loading to the trunk. Unbalanced eccentric masses are mounted to one axis or two central axes to exert orbital or linear loading, respectively. Rotation of two opposing masses reversely, as shown in Fig. 4, could provide linear adjustable loading with maximum capacity of 30,000 N. In other words, the cyclic radial force will be converted to linear reciprocal force using two unbalanced eccentric masses and two rotating shafts in opposite directions around a telescopic central axis. The frame and shaking jaws could rotate at least 200° around the normal axis of the frame surface to provide the grabbing capability of different trunks grown at different angles. To avoid peeling the bark, the jaws were equipped with polymeric pads which damp the sudden impact shocks when shaking linearly. The jaws tightly grab the trunk using hydraulic pressure; thus the shaker is integrated with the tree in the simulation model and defined as an analytical rigid body. There would be higher efficiency when the trunk is smaller in diameter, because of better clamping operation. The flow rate of hydromotor was regulated such that excitation frequencies (rotational speeds) were off the natural frequency of the trunk. In order to conduct the field experiments in a dense olive orchard, a group of similar trees were selected in November with ripe fruits. Then we tried different parameters such as vibration frequency, load directions (linear and orbital), loading height (0.8–1.1 m) – the height at which the trunk is grabbed by the shaker and the load is applied – and tem-

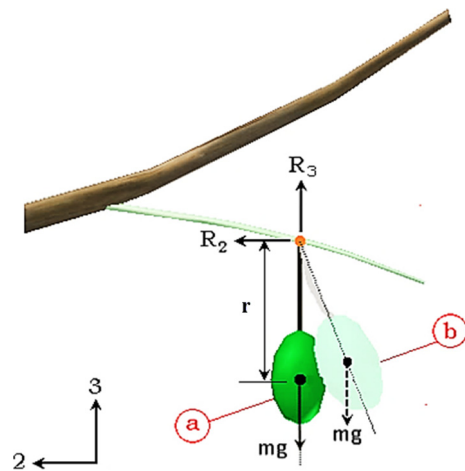


Fig. 6. Free load diagram for olive stem joint on pedicle. (a) Initial position, and (b) after displacement.

perature (10–28 °C) within 10 s. Finally, the HP was calculated using the Eq. (11) (Erdoğan et al., 2003).

$$P_r(\%) = \frac{m_r}{m_r + m_u} \times 100 \quad (11)$$

$P_r$  is the harvested olive percentage,  $m_r$  is the mass of harvested olives and  $m_u$  is the mass of remained fruits on the tree (Sessiz and Özcan, 2006; Erdoğan et al., 2003). Short time duration of shaking is not enough to get all fruits dropped down due to attenuation of transmitted vibrational waves. On the other hand, long vibration time leads to severe loss of leaves and damage to small twigs.

#### 5. Results and discussion

In the first step, A few olive trees of different sizes were dynamically analyzed according to the dimensions mentioned in Table 1. The main modes of vibration are much more affected by the trunk diameter rather than branch size and crown volume. The dynamic response for the minimum and maximum sizes are illustrated in Fig. 8. The results show that displacements on the designated nodes becomes greater when tree size grows up due to an increase of elastic deformation of top branches. However, the difference is not noticeable for olive trees. Therefore, a middle-size tree could be potentially considered as the presentative for the whole to approach to optimum harvesting parameters. For open-center sparse huge canopies of other trees, this phenomenon increases the phase difference between the shaker acceleration vector (force exertion spot) and that of for small branch-twig-stem systems. It would adversely affect the normal stress at most stem-twig joints.

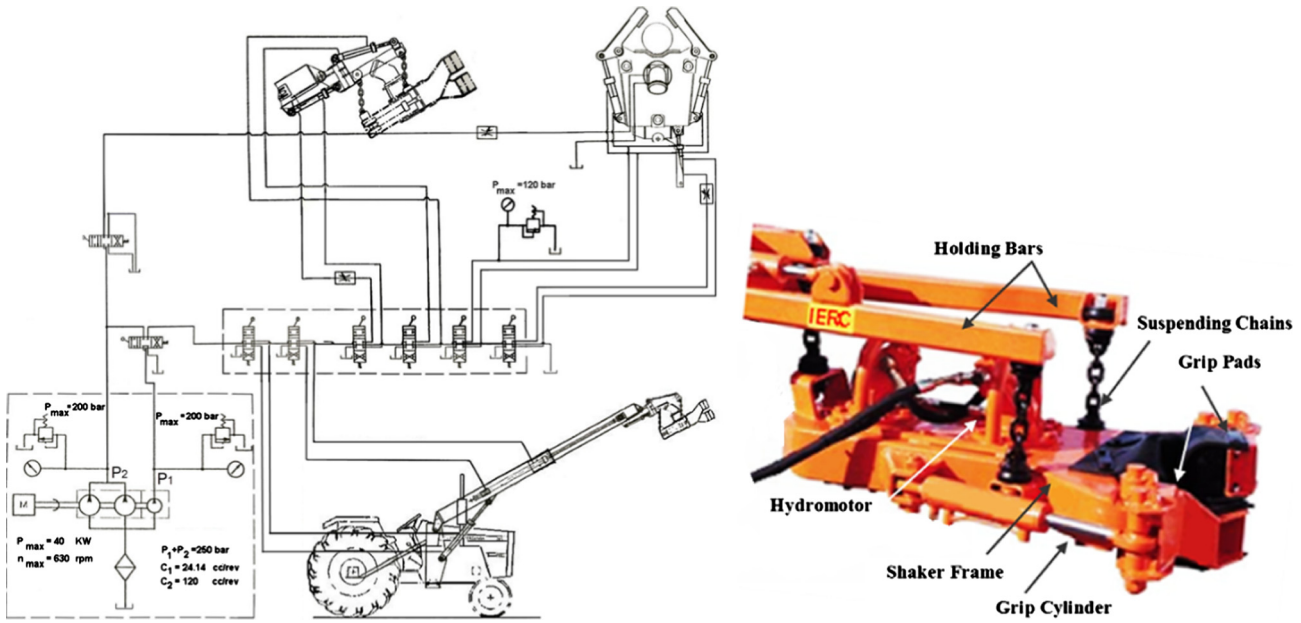


Fig. 7. Configuration of proposed inertial trunk shaker and its hydraulic circuit.

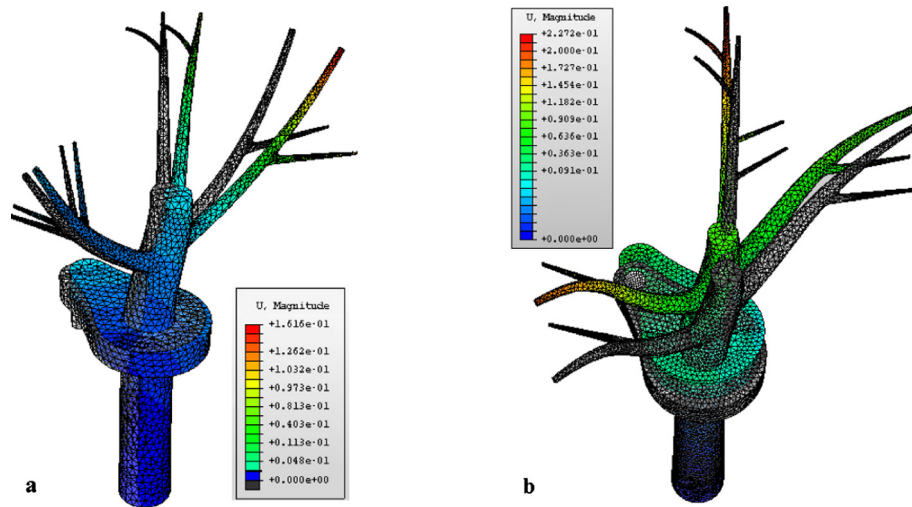


Fig. 8. Displacement due to a 28.9 kN cyclic rotational load exerted to two olive trees, (a) min. size and (b) max. size according to Table 1; at  $f = 20$  Hz and  $T = 20$  °C.

Modal analyses of the middle-size tree and olive structure have been shown separately in Fig. 9 at three main modes of vibration. The three first modes show structural bending and torsion. Thus, considering the critical damping coefficient as  $C_c = 2m\omega_n$ , the damping ratios of the system ( $\zeta = C/C_c$ ) are derived for the first five vibration modes according to Table 2. Numerical results for vibration analysis of orthotropic structure of an olive tree at four stem-twig joints, shown previously in Fig. 1, has been illustrated in Fig. 10 for  $h = 1$  m. There is an initial offset displacement value around which each stem node is oscillating. The offset is caused by the eccentric gravitational force of unbalanced masses relative to the trunk axis. Vibration stress analysis is a suitable method to determine probability of olive detachment at stem-twig nodes in this study. Fig. 11 shows the tension stress at four nodes during the shaking based on Wu-Scheublein yielding criterion parallel to stem fibers direction investigated in the literature (Farinelli et al., 2012b). The FDF can be calculated using these diagrams in excitation bandwidth from 10 to 25 Hz. If the cross section of typical

olive stem is supposed to be  $3.14 \text{ mm}^2$ , the exerted force at a sample node No. 5216 (with lowest stress) is reached to max. 0.24 N at  $f = 10$  Hz, 1.57 N at  $f = 16.5$  Hz, 2.33 N at  $f = 20$  Hz and 2.42 N at  $f = 25$  Hz with respect to maximum stress values of 0.075, 0.5, 0.74 and 0.77 MN/m (MPa), respectively. The stress at other three stem nodes is pretty greater; it has been obtained for node (d) at similar frequency range equal to 0.56, 4.4, 5.8 and 7.17 N considering the maximum stress of 0.18, 1.4, 1.86, and 2.28 MPa. From Figs. 10 and 11, it could be found that for  $f = 16.5$  Hz which trunk resonance phenomenon would be occurred, the stress and displacement quantities increase up to rather 10 times and 5 times respectively, as much as those measured at  $f = 10$  Hz. However, the rising slope of stress tends to lessen as the frequency increases, so that the peak stress value in node 5216—with least stress where we primarily expected not to pick up the necessary detachment force—raised to 0.82 MPa at  $f = 25$  Hz.

It causes 2.58 N nodal force, which is sufficient for a great deal of large olives to be dropped down. Moreover, mean displacement

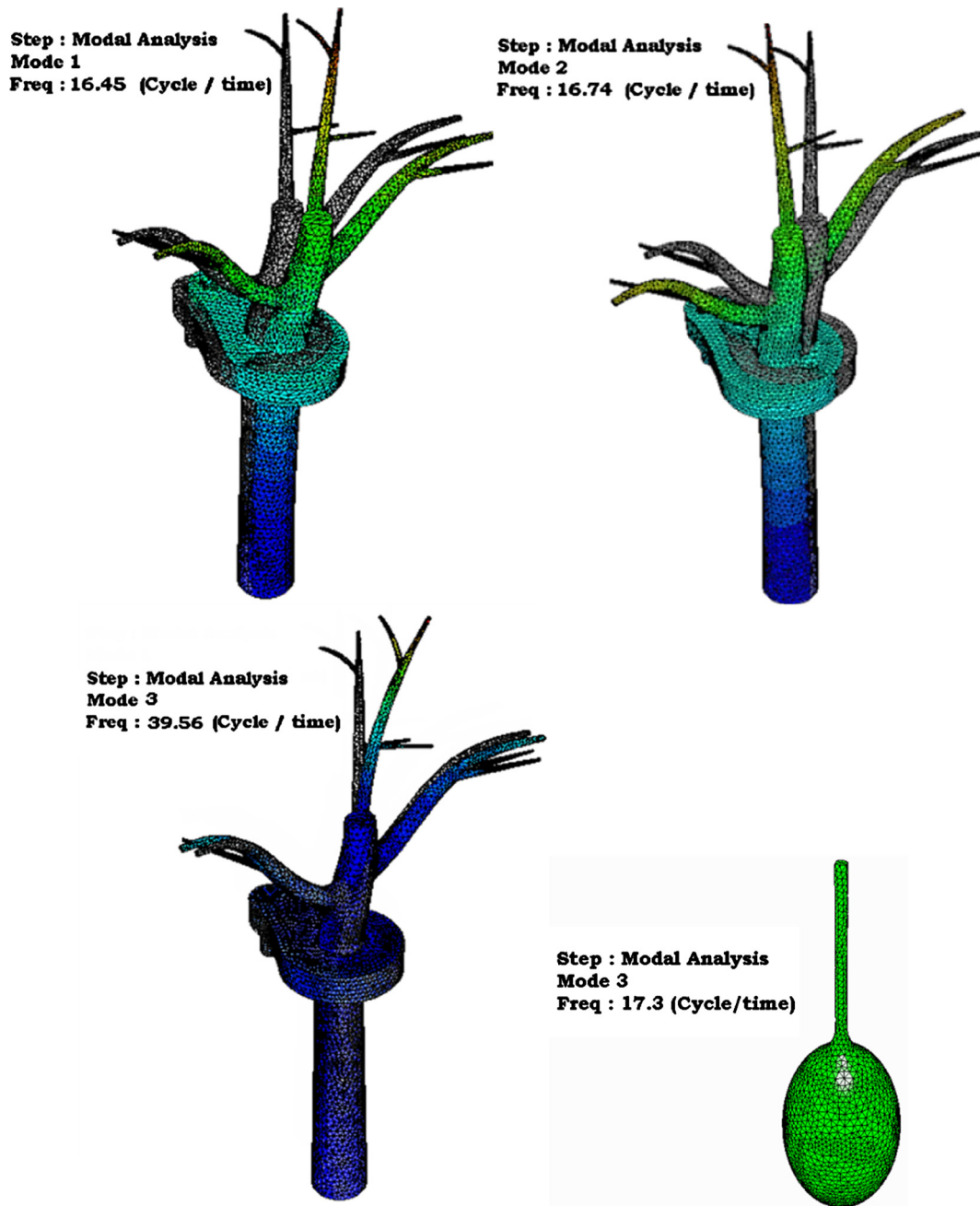


Fig. 9. Modal analysis of olive tree (modes 1, 2, and 3) and olive fruit.

**Table 2**  
Natural frequencies and damping ratios for the first five vibration modes of the olive tree.

	First	Second	Third	Fourth	Fifth
Frequency	16.45	16.74	39.56	41.68	45.5
Damping ratio	0.291	0.286	0.135	0.115	0.108

at all nodes decreases as frequency passes 16.5 Hz. At frequencies of 20 and 25 Hz, the peak-to-peak moderate displacement ( $U_{p-p}$ ) for the four nodes converges to 0.07 and 0.18 m, respectively. Although  $f=25$  Hz shows larger movement, its induced stress at stem nodes is not so tangibly different as the corresponding value for  $f=20$  Hz. So, the lower  $U_{p-p}$  would be preferred to avoid any rupture. It exerts a great force to the trunk, which damages the root and is not an optimum choice.

At lower frequencies, the nodes located far from the trunk and canopy center show higher displacement than the central leads; it demonstrates lower HP and productivity. In Fig. 12, the effect of loading height on the vibration behavior of stem nodes has been recorded at the heights of 0.8, 0.9 and 1.1 m from the ground. The graphs indicate that wave propagation in tree structure will be facilitated with increasing the loading height, which leads to a significant decrease in driving force. The min. peak stress

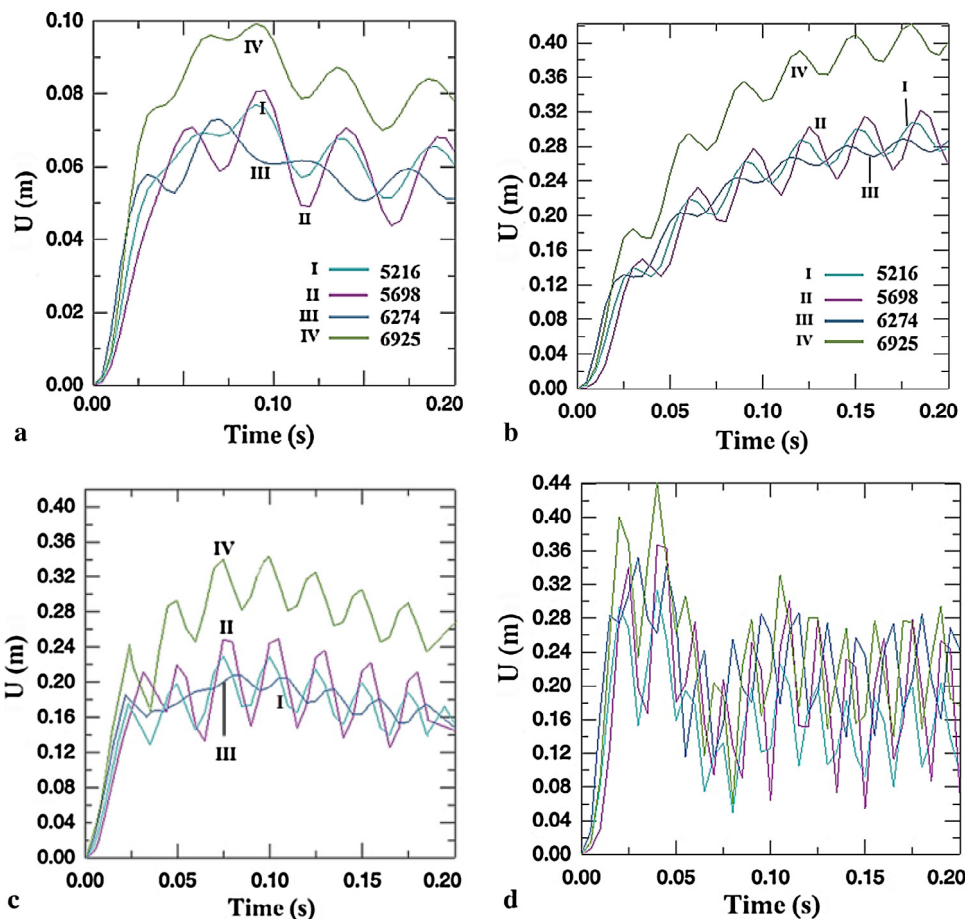


Fig. 10. Displacement at four stem nodes, (a)  $f = 10$  Hz,  $F_r = 7226$  N, (b)  $f = 16.5$  Hz,  $F_r = 19,673$  N, (c)  $f = 20$  Hz,  $F_r = 28,905$  N, (d)  $f = 25$  Hz,  $F_r = 45,163$  N. ( $h = 1$  m).

values—out of four sample nodes—extracted for nodes (d) and (a) (0.11 and 0.19 MPa, respectively) for  $h = 0.8$  m, had a sensible rising trend to be 1.6 and 3.47 MPa for  $h = 1.1$  m which yields 5.1 and 10.9 N tension force, respectively. Further increase in loading height is not safe and allowable, because it will be followed by an exceeded displacement and shear stress at notches and subsequently a breakage would be taken place. Figs. 13 and 14 show variations of displacement and stress at stem node “a” as a function of frequency and loading height. Node “a” stands for the node number 5216 in Fig. 1 which is a pivotal node—close to central axis—in terms of productivity and harvest rate. Although some peaks occur at  $f = 16.5$  and  $f = 25$  Hz, they are not considered as safe frequencies for mechanized harvesting. In Fig. 15, the effect of temperature on the displacement rising of olive nodes has been shown at  $f = 20$  Hz and  $h = 1.1$  m. It’s mainly due to the reduction of elastic modulus and viscous damping with increasing the temperature; the subsequent reduction of relative MC could be obviously realized. Regarding the trivial dimensional variations of trees in the experiments, it could be assumed that the coefficient of thermal expansion (CTE) does not significantly contribute the vibrational behavior of the olive wood at this limited range of temperature variations; However, temperature variations initially affect the MC and eventually the total stress at the stem nodes. By applying a linear load, the stress at the stem nodes increases to approximately 1.5 times as much as that of in orbital loading which affects the harvesting rate; but displacement does not change significantly (Fig. 16(a)). In reference to linear loading, the minimum acceleration magnitude of olive fruit is equal to  $2560$  m/s<sup>2</sup> at 20 Hz, as depicted in Fig. 16(b), that is about 3.25 times greater than the

mean acceleration in similar situation when radial force is applied. Using Newton’s second law of motion and Fig. 16(b), the minimal supporting load ( $R$ ) in the case of linear loading at the position marked by a red<sup>1</sup> circle, is obtained equal to 8.45 N that is 3.12 times as much as 2.7 N derived in rotational loading method. Short shaking duration less than 6 s resulted in a low productivity with a great amount of olives still remained on the tree. Longer than 10 s shaking leads to a likely damage to the bark, small branches, leaves and roots. Experiments show that the most suitable shaking time for this type of olive trees is about 8–10 s. The best harvesting efficiency is obtained when the trunk has a minimum displacement and stem joints have a maximum stress to acceleration ratio. In numerical simulation, the average ratio throughout the canopy determined the HP. To determine practically the harvesting rate, the weight of picked fruits and the rest fruits remained on the tree are measured, separately. Comparing the results with data extracted from manual harvesting method, mechanized harvesting efficiency is obviously revealed. A comparison between FEA results and field experiments of mechanized olive harvesting has been presented in Table 3 as well as in Table 4 at different frequencies regarding the other effective parameters. For both processes, the time duration is equal to 10 s and the tree size is according to the dimensions given in Table 1. Fig. 17 shows the HP variations against the input parameters: temperature, frequency, load direction, and loading height. For  $f < 16.6$  Hz,  $T < 20$  °C and  $h < 1$  m, the difference between linear and

<sup>1</sup> For interpretation of color in Fig. 16, the reader is referred to the web version of this article.

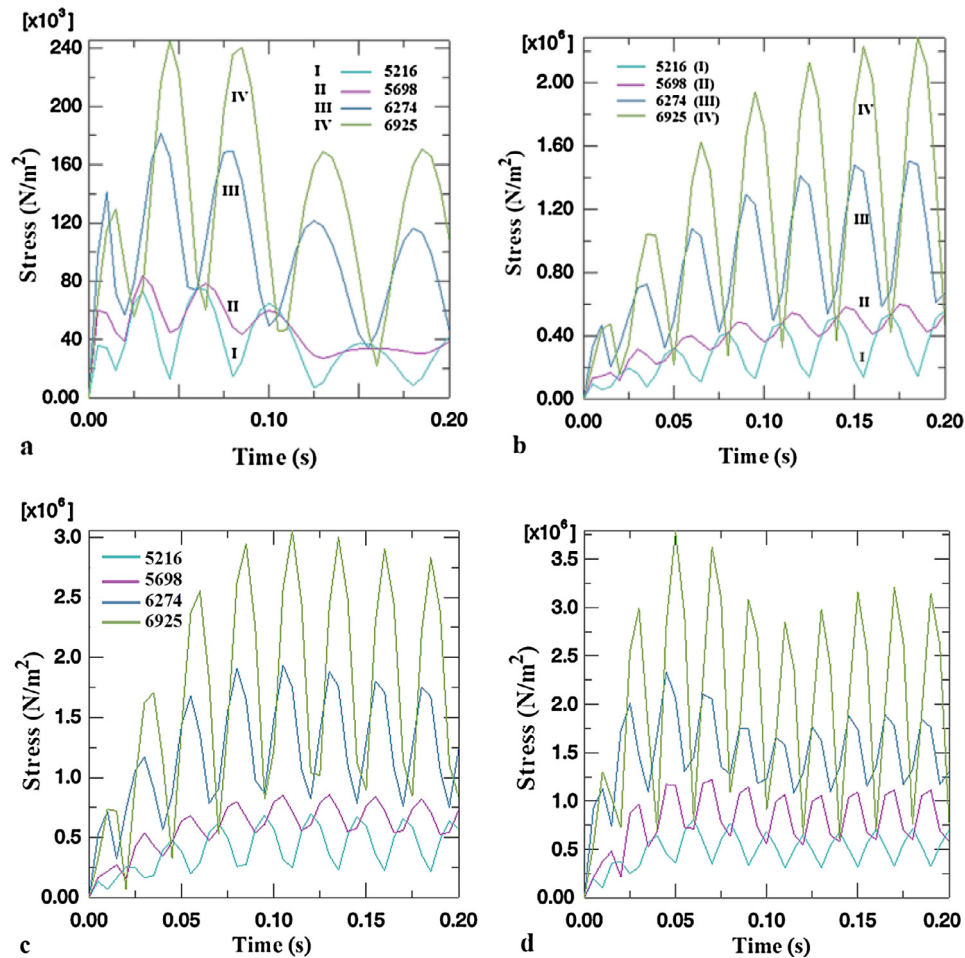


Fig. 11. Stress at four stem nodes, (a)  $f = 10$  Hz,  $F_r = 7226$  N, (b)  $f = 16.5$  Hz,  $F_r = 19,673$  N, (c)  $f = 20$  Hz,  $F_r = 28,905$  N, (d)  $f = 25$  Hz,  $F_r = 45,163$  N. ( $h = 1$  m).

orbital loading could be ignored while the influence of the load direction will be much more perceptible by increasing all effective parameters. Fig. 18(a) shows the variations of experimental HP at highest harvesting rate condition for the 30 olive tree samples. At the beginning of harvest season, the picked quantity does not exceed 50%. In late November 2012 in a sunny day, the best time for harvesting, the olives were mostly ripe. During the experiments, the detachment force-to-weight ratio gradually decreased within a period from nearly 200 (at the beginning) to 45 (at the end of the period). The detachment force was measured about 3–4 N on average in experiments. The 2–3 g light small olives, which freely oscillate synchronized to the vibrating waves propagated into the limbs and small branches, show more detachment resistance than the heavier fruits greater than 4 g. The average productivity per worker reached to about 293 kg/h (~12 tree/h) for  $f = 20$  Hz, and  $T = 28$  °C using linear actuating at  $h = 1.1$  m which is a significant improve in harvesting efficiency. This value is comparable to max. productivity of 71 kg/h reported in (Yousefi et al., 2010; Yousefi and Gholiyan, 2013) for Zard olive cultivar harvested by branch shaker using 4000 ppm ethephon agent in a dense layout orchard. It could be also compared to the harvesting rates reported by Di Vaio et al. (2012) for Orlice and Ortolana cultivars (302 and 246 kg/h, respectively) and those obtained by Famiani et al. (2014) for Cellina Di Nardo (103 kg/h). Although stimulation of the tree at  $f = 20$ –25 Hz, resonates neither the tree structure nor the “olive + stem” system, the displacement of the twigs and small branches are noticeable in the

excitation bandwidth compared to the tree with larger damping losses. Therefore, in the aforementioned range, we expect the olive oscillations and detachment with less trunk movement, as less displacement is more probable specifically in the lower part of the tree, which might be accompanied by less root damages. Comparing the values of Tables 3 and 4 associated to orbital vs. linear loading and temperatures below vs. above 20 °C, it is evident that linear actuating is preferable in our analysis specifically when it is used at the temperatures above 20 °C. Loading height of 1.1 m is also a serious efficacious parameter. In spite of some simplifications in damping and FDF calculations, the discrepancies between the modeled and measured outcomes are hopefully negligible. By implementing statistical analysis, the influence of input parameters was studied on HP using Spearman Correlation method. Table 5 reports the number of experiments (No.), mean value (Mean), standard deviation (SD), minimum (Min) and maximum (Max) quantities of HP for both linear and orbital loading techniques. Table 5 also includes the correlation coefficients among three independent inputs and the HP as the output. The correlation results depicted in Fig. 18(b) show that loading height and frequency are the most effective input parameters, respectively, in both linear and orbital loading states. The loading frequency has a more noticeable influence when the tree is shaken linearly. Temperature mostly shows its complementary influence on HP at orbital loading state where the fruit acceleration and detachment stresses are significantly lower than those at linear loading condition.

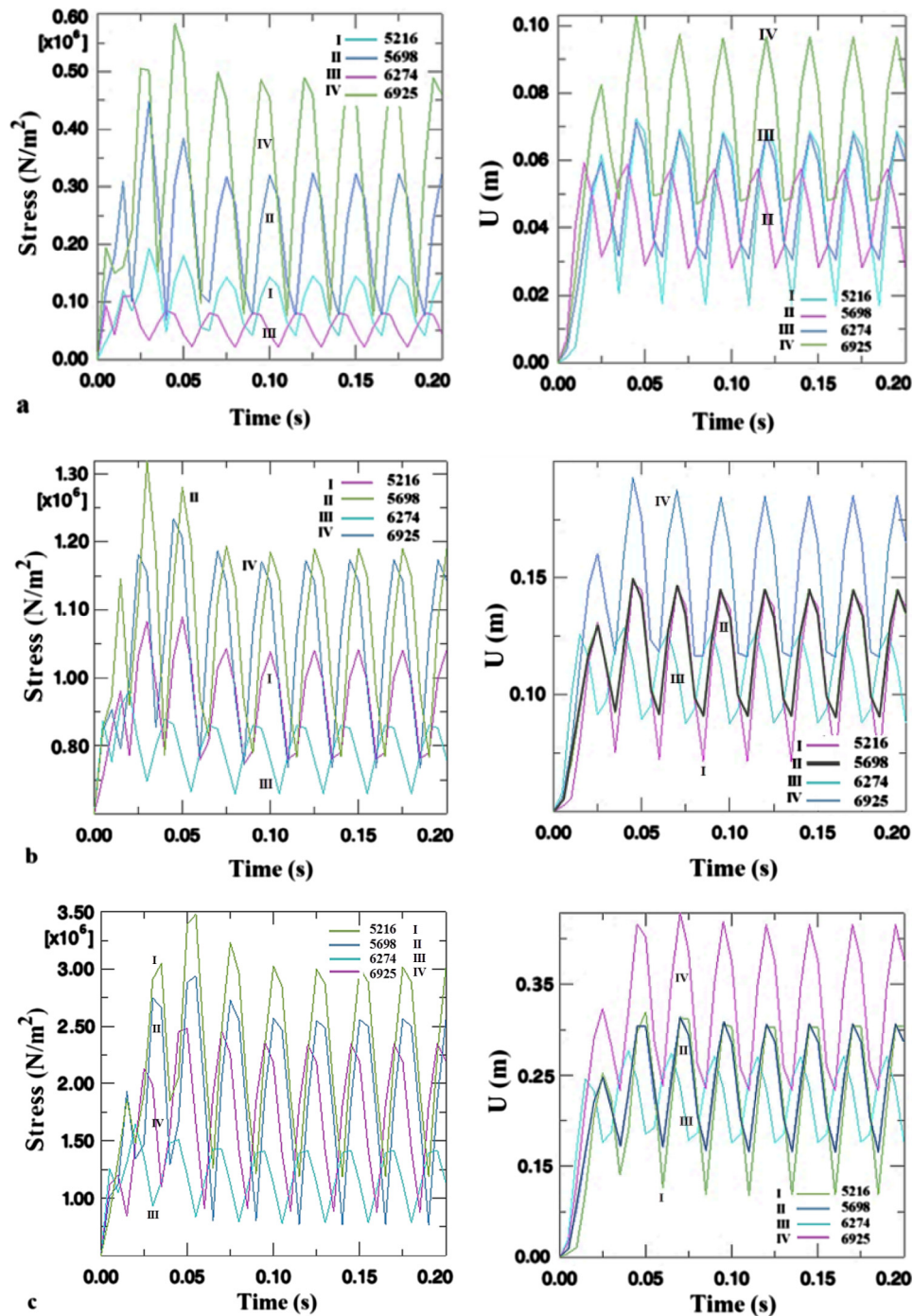


Fig. 12. Stress and displacement variations in four stem nodes at  $f = 20$  Hz and  $T = 23$  °C, for loading height ( $h$ ): (a) 0.8 m, (b) 0.9 m, and (c) 1.1 m.

## 6. Conclusions

The experiment results show that the assumption of dominant root-soil damping with normal eigenmodes is not far away reality for a middle-size olive tree. In conclusion, harvesting at  $f = 20$  Hz in a warm condition (e.g. at noon on a sunny and hot day with  $T = 28$  °C) for 10 s when the shaker mounted on 1.1 m above the ground, resulted in the greatest harvesting efficiency in simulations validated by field experiments. The highest percentages of 96% and 92% were achieved for FEA and experimental tests, respectively. While the maximum HP of the orbital loading are 80% and 82% for FEM and experiments, respectively, linear actuating shows

a noticeable enhancement in the picked crop mass by 16% and 10% at the same conditions as considered for the orbital loading. It is also found that at  $h = 1.1$  m a uniform vibratory wave is propagated throughout almost all canopy volume, having a positive impact (5.7% increase) in harvest efficiency compared to  $h = 1$  m. Practically, olive HP and productivity at  $T = 28$  °C increased by 2.3% and 8.5%, relative to 20 and 15 °C. The natural frequency of “fruit-stem” is a key criterion in the design of mechanical vibratory harvesting device, in which the maximum displacement and stress amplitude occurred at the stem nodes that facilitates fruit detachment, while avoiding of damage formation in trunk and branches. Oscillatory waves in hard dry wood are more easily transmitted to

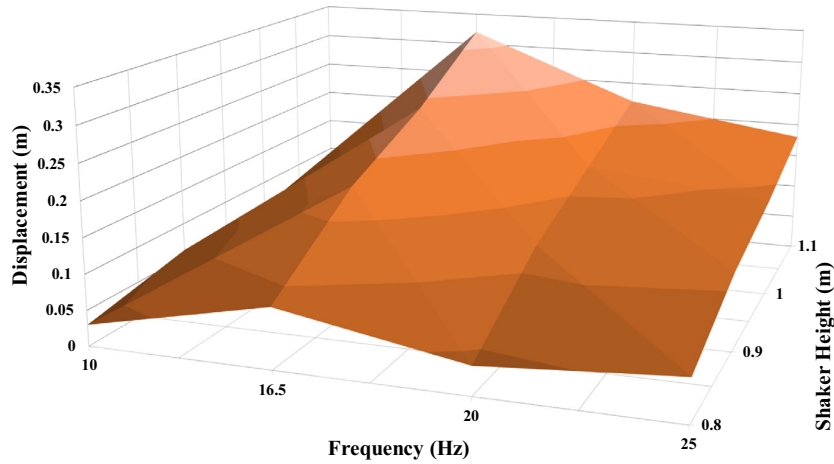


Fig. 13. Displacement of node "a" vs. frequency and loading height. ( $T = 23\text{ }^{\circ}\text{C}$ ).

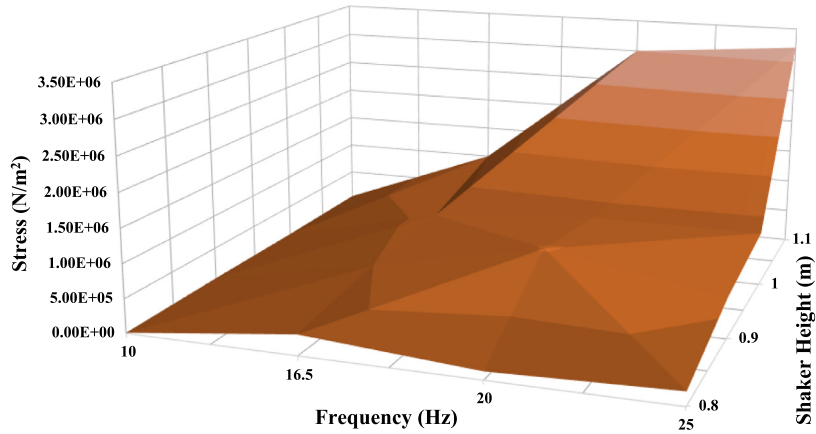


Fig. 14. Stress at node "a" vs. frequency and loading height at  $T = 23\text{ }^{\circ}\text{C}$ .

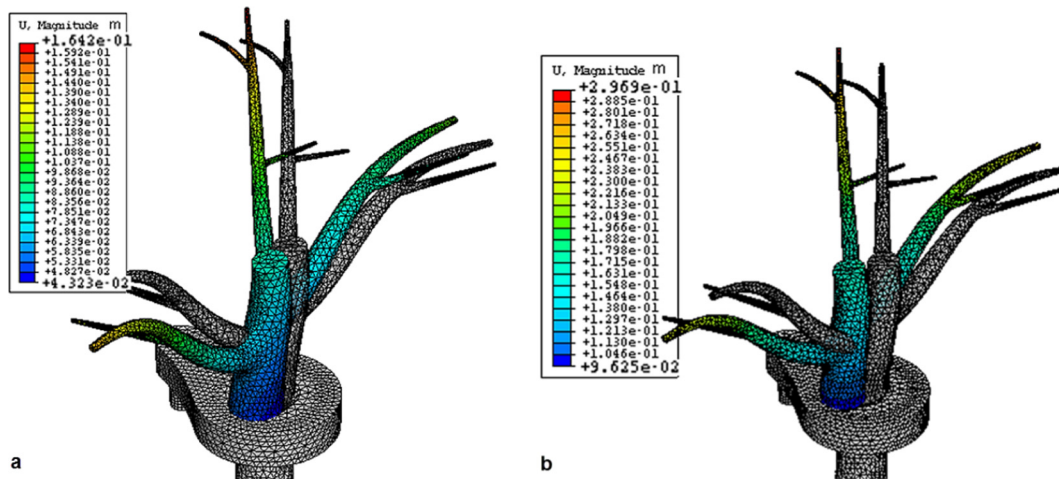
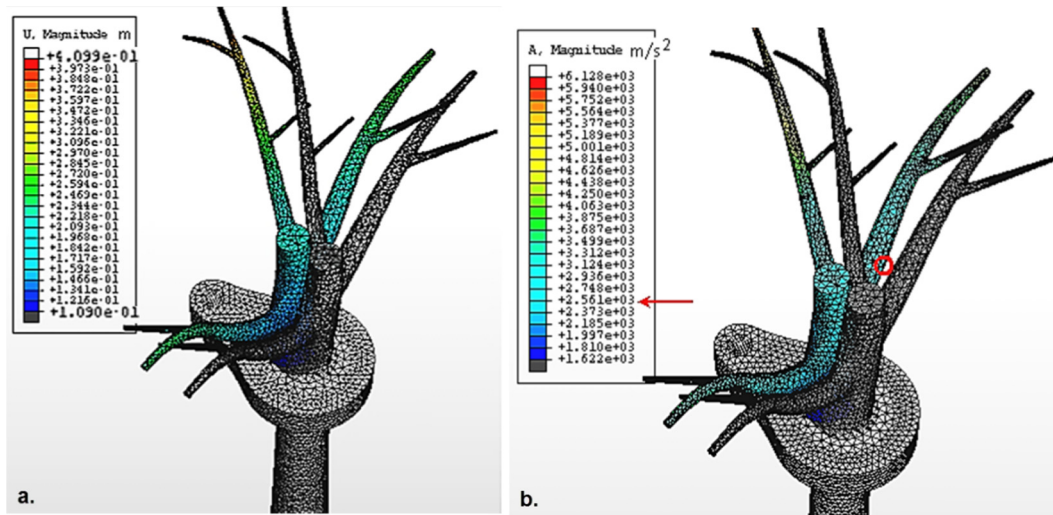


Fig. 15. Temperature effects on displacement of stem nodes at (a)  $T = 15\text{ }^{\circ}\text{C}$  and  $\text{MC} = 51\%$ , and (b)  $T = 28\text{ }^{\circ}\text{C}$  and  $\text{MC} = 45\%$ . ( $f = 20\text{ Hz}$ ).

small branches at higher temperatures in which the humidity is lower. Wood defects such as knots and notches affect severely the tensile and bending strength as well as endurance limit. This is one of the most important reasons for differences between simulation and field experiment results. However, less than 5% difference reveals the importance of dynamic analysis of a tree to

improve adjusting parameters. The 3D model of this case study could also be deployed to other olive cultivars, not limited to *Mari* cultivar, with little modifications in physical and damping characteristics. The methodology of developing efficient dynamic modeling is economically affordable for those types of olive trees which are regularly planted and pruned. Statistical analysis shows



**Fig. 16.** (a) Displacement derived from a 28.9 kN cyclic linear load exerted at  $f = 20$  Hz and  $T = 28$  °C (MC = 45%), and (b) acceleration of olive fruit attached to stem joints (linear loading).

**Table 3**  
Olive harvesting percentage, comparison of FEA (A) with field experiment results (B), for variant temperatures and loads.

	Freq. (Hz)	$T = 20$ °C, $h = 1$ m		$T = 28$ °C, $h = 1$ m													
		Load direction		Linear			Orbital										
		Linear	Orbital														
A	10	57	48		62				50								
	16.5	73	65		75				63								
	20	83	75		86				77								
	25	90	78		92				-								
B	10	65	58	$HP^a \pm 1\%$	$M^b \pm 1\%$	$SD^c$	$HP \pm 1\%$	$M \pm 1\%$	$SD$	60	65	3.59	51	57	4.20		
										66			56				
										67			58				
										68			61				
	16.5	74	71			3.32			73	73	3.55	73					
												76			75		
												80			76		
	20	87	75			2.50			77	75	3.51	85					
												87			73		
												90			76		
	25	89	78			2.22			80			91					
												92					
												93					

<sup>a</sup> Triple repetition of harvesting percentage (HP) measurement on similar trees.

<sup>b</sup> Mean value (M).

<sup>c</sup> Standard deviation (SD).

**Table 4**  
Olive harvesting percentage, comparison of FEA (A) with field experiment results (B), for variant temperatures and loading heights.

	Freq. (Hz)	$T = 15$ °C, linear loading $h = 1$ m	$T = 28$ °C, linear loading $h$ (m)		
			0.8	0.9	1.1
A	10	58	42	56	67
	16.5	68	48	64	79
	20	71	62	77	96
	25	75	64	78	-
B	10	60	45	53	68
	16.5	64	51	64	78
	20	70	65	73	92
	25	77	63	82	-

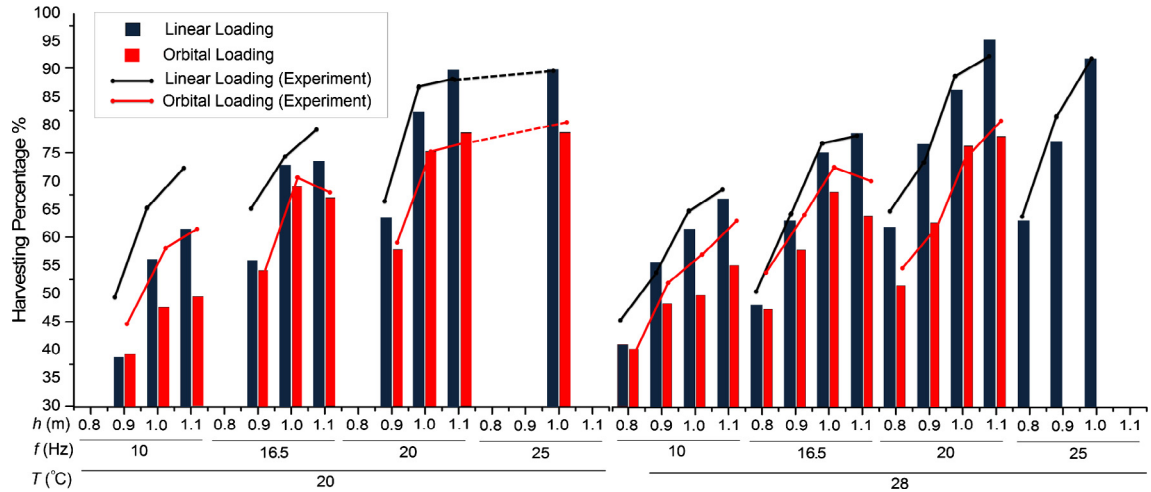


Fig. 17. Harvesting percentage vs. temperature, frequency, loading height and loading direction.

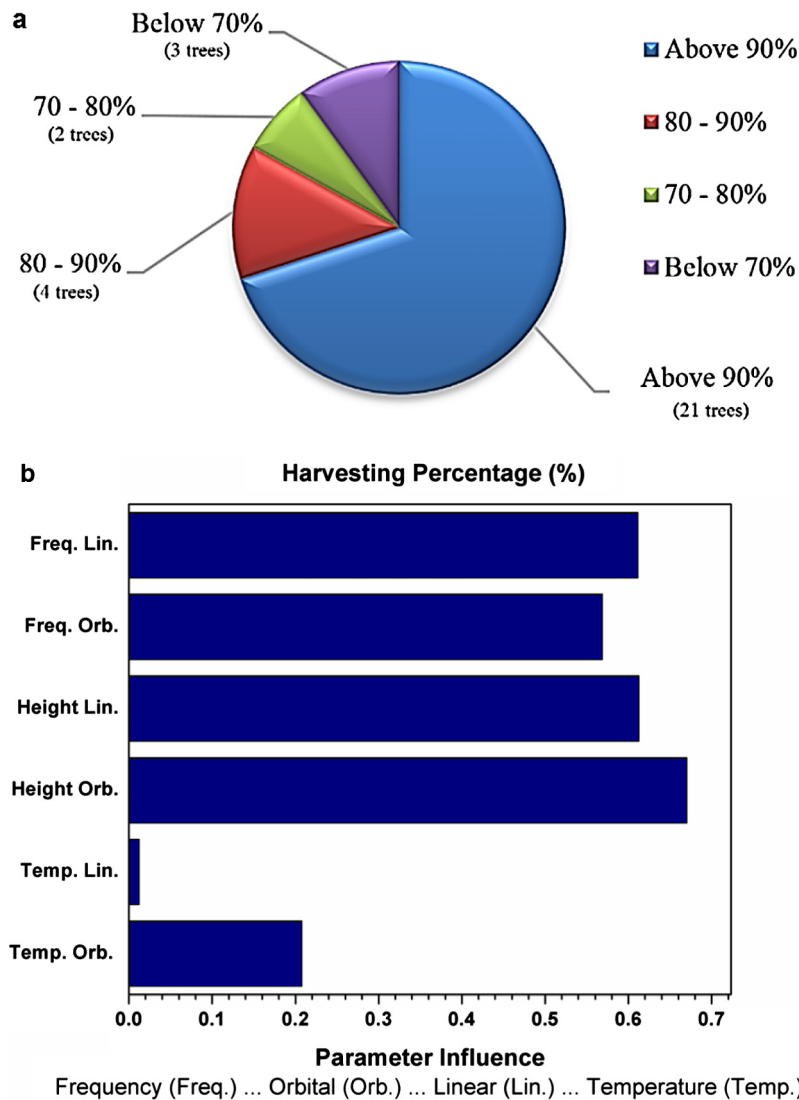


Fig. 18. (a) Variations of experimental HP at  $f = 20$  Hz for linear loading,  $T = 28$  °C,  $MC = 45\%$  and  $h = 1.1$  m, and (b) comparison of parameters influence on HP (%) at linear and orbital loading conditions.

**Table 5**  
Spearman correlation coefficients taken for harvesting percentage.

		Linear loading	Orbital loading
HP (%)	No.	30	30
	Mean	61.2	71.14
	SD	10.72	12.97
	Min-Max	39–82	45–92
	HP Correlation Coefficients		
Temperature (°C)		0.0121	0.2075
Loading height (m)		0.6126	0.6698
Frequency (Hz)		0.6111	0.5685

larger HP mean value of linear loading than shaking orbitally as well as different influence of input parameters on HP. Loading height is considered as the most effective parameter beside the loading frequency which shows a more noticeable influence in linear approach. Temperature has not significant effect on HP when linear method is applied and it could be interpreted based on the high impact of linear forces on fruit acceleration and detachment stresses at stem–twig joints.

### Acknowledgement

The research did not receive any specific grant from funding agencies in the public, commercial, or not-for-profit sectors.

### References

- Adrian, P.A., Fridley, R.B., 1965. Dynamics and design criteria of inertia-type tree shaker. *Trans. ASAE* 8, 12–14.
- Bentaher, H., Haddar, M., Fakhfakh, T., Mäalej, A., 2013. Finite elements modeling of olive tree mechanical harvesting using different shakers. *Trees Struct. Funct.* 27, 1537–1545.
- Bower, A.F. (Ed.), 2009. *Applied Mechanics of Solids Hardcover*. CRC Press, Taylor & Francis Group, New York, USA.
- Bucur, V. (Ed.), 2006. *Acoustics of Wood. 2*. Springer-Verlag, Berlin-Heidelberg, Germany.
- Castro-García, S., Blanco-Roldán, G.L., Gil-Ribes, J.A., Agüera-Vega, J., 2008. Dynamic analysis of olive trees in intensive orchards under forced vibration. *Trees Struct. Funct.* 22, 795–802.
- Castro-García, S., Castillo-Ruiz, F.J., Jimenez-Jimenez, F., Gil-Ribes, J.A., Blanco-Roldán, G.L., 2015. Suitability of Spanish 'Manzanilla' table olive orchards for trunk shaker harvesting. *Biosyst. Eng.* 129, 388–395.
- Castro-García, S., Castillo-Ruiz, F.J., Sola-Guirado, R.R., Jiménez-Jiménez, F., Blanco-Roldán, G.L., Agüera-Vega, J., Gil-Ribes, J.A., 2014. Table olive response to harvesting by trunk shaker. In: *Proceedings of the International Conference of Agricultural Engineering*, 6–10 July 2014, Zurich.
- Chowdhury, I., Dasgupta, S.P., 2003. Computation of Rayleigh damping coefficients for large systems. *Elec. J. Geotech. Eng.* 8.
- Cicek, G., Sumer, S.K., Kocabiyik, H., 2010. Effect of different harvest methods on olive yield and work capacity. *Afr. J. Agric. Res.* 5, 3246–3250.
- Dahmen, S., Ketata, H., Ben Ghazlen, M.H., Hosten, B., 2010. Elastic constants measurement of anisotropic Olivier wood plates using air-coupled transducers generated Lamb wave and ultrasonic bulk wave. *Ultrasonics* 50, 502–507.
- Di Vaio, C., Marallo, N., Nocerino, S., Famiani, F., 2012. Mechanical harvesting of oil olives by trunk shaker with a reversed umbrella interceptor. *Adv. Hort. Sci.* 26, 176–179.
- Di Vaio, C., Nocerino, S., Paduano, A., Sacchi, R., 2013. Characterization and evaluation of olive germplasm in Southern Italy. *J. Sci. Food Agric.* 93, 2458–2462.
- El-Awady, M.N., Genaidy, M.A.I., Rashowan, M., El-Attar, M.Z., 2008. Modeling and simulating of olive-tree harvesting mechanism. *Misr. J. Agric. Eng.* 25, 712–722.
- Erdoğan, D., Güner, M., Dursun, E., Gezer, I., 2003. Mechanical harvesting of apricots. *Biosyst. Eng.* 85, 19–28.
- Famiani, F., Farinelli, D., Rollo, S., Camposeo, S., Di Vaio, C., Inglese, P., 2014. Evaluation of different mechanical fruit harvesting systems and oil quality in very large size olive trees. *Span. J. Agric. Res.* 12, 960–972.
- Farinelli, D., Ruffolo, M., Boco, M., Tombesi, A., 2012a. Yield efficiency and mechanical harvesting with trunk shaker of some international olive cultivars. *Acta Hort.* 949, 379–384.
- Farinelli, D., Tombesi, S., Famiani, F., Tombesi, A., 2012b. The fruit detachment force to fruit weight ratio can be used to predict the harvesting yield and efficiency of trunk shakers on mechanically harvested olives. *Acta Hort.* 965, 61–64.
- Ferguson, L., Rosa, U., Castro-García, S., Lee, S.M., Guinard, J.X., Burns, J., Krueger, W. H., O'Connell, N.V., Glozer, K., 2010. Mechanical harvesting of California table and oil olives. *Adv. Hort. Sci.* 24, 53–63.
- Gezer, I., 1999. Determination of relationships between spring rigidity and some other tree properties in apricot trees with respect to harvesting technique. *Turk. J. Agric. For.* 5, 1065–1069.
- Green, D.W., Evans, J.W., 2008. The immediate effect of temperature on the modulus of elasticity of green and dry lumber. *Wood Fiber Sci.* 40, 374–383.
- Hedden, S.L., Churchill, D.B., 1984. Orange removal with trunk shakers. *Proc. Fla. State Hort. Soc.* 97, 47–50.
- Horvath, E., Sitkei, G., 2001. Energy consumption of selected tree shakers under different operational condition. *J. Agric. Eng.* 80, 191–199.
- James, K.R., Haritos, N., Ades, P.K., 2006. Mechanical stability of trees under dynamic loads. *Amer. J. Bot.* 93, 1522–1530.
- Keçecioglu, G., 1975. Research on Olive Harvesting Possibilities with an Inertia Type Shaker MSc. Ege University, İzmir, Turkey.
- Khandan, R., Noroozi, S., Sewell, P., Vinney, J., 2012a. The development of laminated composite plate theories: a review. *J. Mater. Sci.* 47, 5901–5910.
- Khandan, R., Noroozi, S., Sewell, P., Vinney, J., Koohgilani, M., 2012b. Optimum design of fibre orientation in composite laminate plates for out-plane stresses. *Adv. Mater. Sci. Eng.* 2012, 1–11.
- Mascia, N.T., 2003. Concerning the elastic orthotropic model applied to wood elastic properties. *Maderas Ciencia Tecnol.* 5, 3–19.
- Mascia, N.T., Cramer, S.M., 2009. On the effect of the number of annual growth rings, specific gravity and temperature on redwood elastic modulus. *Maderas Ciencia Tecnol.* 11, 47–60.
- Mascia, N.T., Lahr, F.A.R., 2006. Remarks on orthotropic elastic models applied to wood. *Mater. Res.* 9, 301–310.
- Metzidakis, M., 1999. Field studies for mechanical harvesting by using chemicals for the loosening of olive pedicel on cv. Koroneiki. *Acta Hort.* 474, 197–202.
- Saglam, C., Aktas, T., 2005. Determination of some physical properties and static friction coefficient of olive. *J. Agron.* 4, 308–310.
- Savary, S.K.J.U., Ehsani, R., Schueller, J.K., Rajaraman, B.P., 2010. Simulation study of citrus tree canopy motion during harvesting using a canopy shaker. *Am. Soc. Agric. Biol. Eng.* 53, 1373–1381.
- Sellier, D., Fourcaud, T., 2005. A mechanical analysis of the relationship between tree oscillations of *Pinus pinaster* Ait saplings and their aerial architecture. *J. Exp. Bot.* 56, 1563–1573.
- Sessiz, A., Özcan, M.T., 2006. Olive removal with pneumatic branch shaker and abscission chemical. *J. Food Eng.* 76, 148–153.
- Sola-Guirado, R.R., Castro-García, S., Blanco-Roldán, G.L., Jiménez-Jiménez, F., Castillo-Ruiz, F., Gil-Ribes, J.A., 2014. Traditional olive tree response to oil olive harvesting technologies. *Biosyst. Eng.* 118, 186–193.
- Yousefi, Z., Almassi, M., Zeinanloo, A.A., Moghadasi, R., Khorshidi, M.B., 2010. A comparative study of olive removal techniques and their effects on harvest productivity. *J. Food Agric. Environ.* 8, 240–243.
- Yousefi, Z., Gholyani, A., 2013. A study of olive harvesting methods in Iran from an economic perspective. *Tech. J. Eng. Appl. Sci.* 3, 1005–1015.
- Yung, C., Fridley, R.B., 1975. Simulation of vibration of whole tree system using finite element. *IEEE Trans. Autom. Sci. Eng.* 18, 475–481.